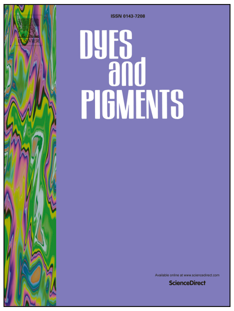

Influence of the structure of electron-donating aromatic units in organosilicon luminophores based on 2,1,3-benzothiadiazole electron-withdrawing core on their absorption-luminescent properties

Maxim S. Skorotetcky, Evgeniya D. Krivtsova, Oleg V. Borshchev, Nikolay M. Surin, Evgeniya A. Svidchenko, Yuriy V. Fedorov, Sergey A. Pisarev, Sergey A. Ponomarenko

PII: S0143-7208(17)32545-7
DOI: 10.1016/j.dyepig.2018.03.043
Reference: DYPI 6628

To appear in: *Dyes and Pigments*

Received Date: 13 December 2017
Revised Date: 21 March 2018
Accepted Date: 21 March 2018

Please cite this article as: Skorotetcky MS, Krivtsova ED, Borshchev OV, Surin NM, Svidchenko EA, Fedorov YV, Pisarev SA, Ponomarenko SA, Influence of the structure of electron-donating aromatic units in organosilicon luminophores based on 2,1,3-benzothiadiazole electron-withdrawing core on their absorption-luminescent properties, *Dyes and Pigments* (2018), doi: 10.1016/j.dyepig.2018.03.043.

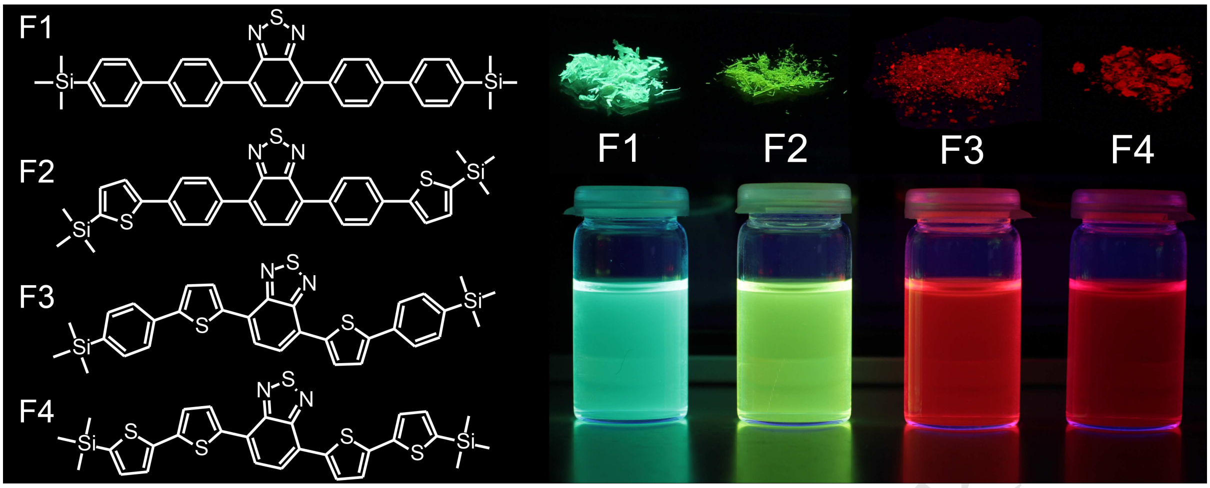
F1
F2
F3
F4
N
S
Si
F1
F2
F3
F4

Influence of the structure of electron-donating aromatic units in organosilicon luminophores based on 2,1,3-benzothiadiazole electron-withdrawing core on their absorption-luminescent properties

Maxim S. Skorotetcky [a], Evgeniya D. Krivtsova[a], Oleg V. Borshchev [a], Nikolay M. Surin [a], Evgeniya A. Svidchenko [a], Yuriy V. Fedorov [b], Sergey A. Pisarev [c], Sergey A. Ponomarenko [a, d] *

[a] *Enikolopov Institute of Synthetic Polymeric Materials of Russian Academy of Sciences, Profsoyuznaya St. 70, Moscow 117393, Russia*

[b] *Nesmeyanov Institute of Organoelement Compounds of Russian Academy of Sciences, Vavilova st. 28, Moscow 119991, Russia*

[c] *Institute of Physiologically Active Compounds of Russian Academy of Sciences, Severny Pr. 1, Chernogolovka 142432, Russia*

[d] *Chemistry Department, Moscow State University, Leninskie Gory 1-3, Moscow 119991, Russia*

**e-mail: ponomarenko@ispm.ru*

Highlights

- Four new organosilicon luminophores based on benzothiadiazole are synthesized
- They possess high efficiency and large Stokes shift in solution and polymer matrix
- An approach to tune their optical properties in wide spectral range is reported
- The nearest donor fragments have the greatest influence on the spectral properties.
- TMS groups accelerate fluorescence, increase solubility and extinction coefficient.

Keywords: organosilicon luminophores, fluorescence, conjugated oligomers, benzothiadiazole, large Stokes shift

A series of new linear π-conjugated oligomers consisting of five conjugated rings based on 2,1,3-benzothiadiazole (BTD) electron-withdrawing group and various combinations of 2,5-thiophene and 1,4-phenylene electron-donating units with terminal trimethylsilyl groups has been synthesized and characterized. Investigation of their absorption-luminescent properties revealed that all of them possess high photoluminescence (PL) quantum yield and large Stokes shift both in diluted solutions and polymer matrix, while in the solid state their PL efficiency decreases. It was found that the main factor influencing the optical properties of the molecules obtained is the type of aromatic fragment directly attached to the central BTD moiety. Changing the chemical structure of the donor aromatic fragments from 1,1'-biphenyl to 2,2'-bithiophene allows tuning the PL spectral maximum of the luminophores in wide range from 510 to 660 nm. It was shown that the presence of trimethylsilyl groups in these luminophores is responsible for their increased solubility, enhanced molar extinction coefficients and shortening the excited state lifetime without decreasing the PL efficiency.

1. Introduction

Luminophores as functional materials are successfully applied in many fields of science and technology. Great progress has been made in the development of various electronic devices based on organic materials such as displays [1,2], organic light-emitting transistors [3–5], luminescent down-shifting layers for photovoltaic [6]. 2,1,3-Benzothiadiazole (BTD) derivatives play an important role among such materials due to their unique optical and electronic properties. They are normally form efficient luminophores [7–11], characterized by high chemical and thermal stability, also widely used in organic photovoltaic materials as strong electron-withdrawing moiety [12,13]. In addition, compounds based on BTD due to their relatively high reduction potential and electron affinity are widely used as emissive layers in organic light-emitting diodes (OLEDs) [14,15].

Typically, BTD-based luminescent materials are symmetrical molecules composed by a donor−acceptor− donor (D-A-D) framework with an electron-poor benzothiadiazole central core connected to two electron-rich substituents. 4 and 7 positions of BTD unit are usually preferred for direct π-extension and has a very positive effect both on PL spectra and photostability [16,17]. More importantly, the absorption-luminescent properties of such molecules can be tuned by the electronic properties of the extended donor substituents [18–20].

On the one hand, high potential of luminescent BTDs derivatives was already demonstrated and recently reviewed [21]. However, there is very little information available about the interactions between the BTD acceptor and various donor substituents. On the other hand, σ-π interactions of the silylene group with the conjugated chromophores is well known [22,23]. Introduction of silicon atoms into conjugated organic compounds can lead to the following advantages: high thermal stability; high solubility in many organic solvents and therefore good processability from solutions, which is necessary for obtaining various devices of organic electronics by inexpensive printing methods; and the most important – the presence of specific electronic effects [24]. These include an increase in the conjugation due to direct influence of silicon on the conjugated system, which is the reason for an increase in the molar extinction coefficient and a shift of the optical spectra maxima to the long-wavelength region [25,26]. In addition, organosilicon luminophores, in contrast to their non-silicon analogues, can exhibit an increased photoluminescence quantum yield (PLQY) [27]. Therefore, organosilicon derivatives of BTD-based luminophores are promising materials both from the fundamental and applied points of view. In this work the synthesis and systematic study of optical and thermal properties of four novel BTD-based luminophores, being linear conjugated oligomers with a conjugation length of five aromatic rings with the central BTD acceptor core containing various combinations of 1,4-phenylene and 2,5-thiophene units with terminal trimethylsilyl (TMS) groups are reported (Fig.1). Influence of the TMS groups on physical properties of the luminophores was revealed by comparing compound **F1** with its full analogue **F1a** without TMS groups described earlier [18,19,28].

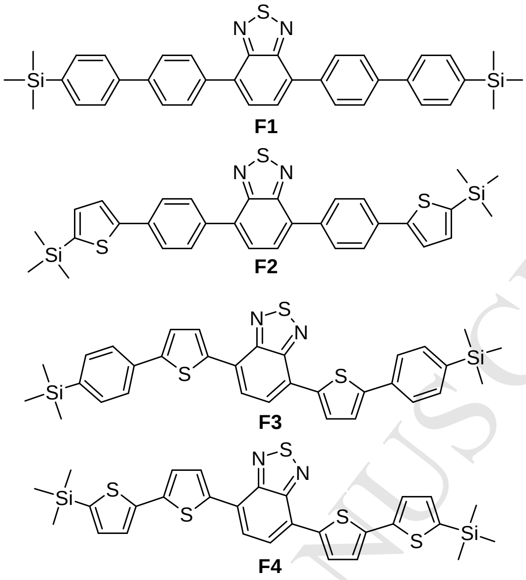

Fig. 1. Chemical structures of novel organosilicon luminophores based on 2,1,3-benzothiadiazole core synthesized and investigated in this work.

2. Experimental section

2.1. Materials

Hexane solutions of 1.6M and 2.5M *n*-butyllithium (CAUTION: solution can ignite in contact with water and carbon dioxide [29], this compound should be handled under nitrogen with special equipment[30]), trimethylchlorosilane (CAUTION: Reacts violently or explosively with water [31,32]), 2-bromothiophene, sodium carbonate, magnesium and 1,4-dibromobenzene were obtained from Acros organics; *tetrakis*(triphenylphosphine)palladium(0) $Pd(PPh_3)_4$, [1,1′-*bis*(diphenylphosphino)ferrocene] dichloropalladium(II), 2-isopropoxy-4,4,5,5-tetramethyl-1,3,2-dioxaborolane (IPTMDOB) were obtained from Sigma-Aldrich and used as received. 2-(4,4,5,5-Tetramethyl-1,3,2-dioxaborolan-2-yl)-5-(trimethylsilyl)-thiophene (**2**) [33], (4'-bromobiphenyl-4-yl)(trimethyl)silane (**3**) [34], trimethyl[4-(2-thienyl)phenyl]silane (**5**), 2,2'-

bithien-5-yl(trimethyl)silane (**6**) [35], trimethyl{4-[5-(4,4,5,5-tetramethyl-1,3,2-dioxaborolan-2-yl)-2-thienyl]phenyl}silane (**9**) [26] and 4,7-dibromo-2,1,3-benzothiadiazole (**11**) [8] were synthesized as described earlier. THF, diethyl ether, toluene and ethanol were dried and purified according to the standard techniques and then used as the solvents.

2.2. Characterization

The ^{1}H NMR spectra were recorded on a Bruker WP250 SY spectrometer (250.13 MHz) using the residual signal of $CDCl_3$ (δ 7.27 ppm) as the internal standard. The ^{13}C and ^{29}Si NMR spectra were recorded on a Bruker Advance II 300 spectrometer at working frequencies 75 MHz and 60 MHz, respectively. In the case of ^{1}H NMR spectroscopy, the compounds to be analyzed were taken in the form of 0.5% solutions in $CDCl_3$. In the case of ^{13}C or ^{29}Si NMR spectroscopy, the compounds to be analyzed were taken in the form of 1-3% solutions in $CDCl_3$. The spectra were then processed on the computer using the ACD Labs software.

Elemental analysis of C, H, N elements was carried out using CHN automatic analyzer CE1106 (Italy). Experimental error is 0.30−0.50%. The burning was done in the Sheninger flask using alkaline solution of hydrogen peroxide as an absorbent. Spectrophotometry technique was used for the Si analysis.

Thermogravimetric analysis was carried out in dynamic mode in 30-800 °C interval using Mettler Toledo TG50 system equipped with M3 microbalance allowing measuring the weight of the samples in 1-150 mg range with 1 µg precision. Heating/cooling rate was chosen to be 20 °C/min. Every compound was studied twice: in air and under nitrogen flow of 200 mL/min.

GPC analysis was performed on a Shimadzu instrument with a RID10A^{VP} refractometer and a SPD-M10A^{VP} diode matrix as detectors using 7.8 × 300 mm^{2} Phenomenex columns (USA) filled with the Phenogel sorbent with pore size of 500 Å and THF as the eluent. In the case of column chromatography, silica gel 60 (“Merck”) was taken. For thin layer chromatography (TLC), "Sorbfil" (Russia) plates were used. The solvents were removed under vacuum (1 mBar) at 80 °C. All reactions, unless stated otherwise, were carried out in an inert atmosphere using anhydrous solvents.

The absorption spectra were recorded on a Shimadzu UV-2501PC (Japan) spectrophotometer in the standard 10 mm photometric quartz cuvette using THF solutions with the concentrations of 10^{-5} M. A scanning spectrofluorimeter ALS01M (Russia) with registration in single photon counting mode at successive time intervals and automatic adjustment of the intensity of the measured emission was used for the registration of photoluminescence spectra (PL). Measurements were carried out for several optical densities in the range from 0.06 to 0.12 absorbance units in 10 mm cuvette, measurement geometry – 90°. Measurements of the PL spectra in polystyrene (PS) and polycrystalline thin films were carried out in the integrating sphere. The photoluminescence quantum yield (PLQY) was measured by comparing the integral PL intensity of 10^{-6} M diluted solutions of luminophores in THF with the integral PL intensity of the standard as described elsewhere [36]. As the standards in measuring the PLQY a solution of 1,4-*bis*(5-phenyloxazol-2-*yl*)benzene (POPOP) in cyclohexane (PLQY=1) and a solution of rhodamine 6G in ethanol (PLQY=1) were used. Measurements of the PL lifetime were made by the pulsed method in single photon counting mode on the Fluorolog-3 spectrofluorimeter (HORIBA Scientific).

Density functional theory (DFT) calculations were performed using the ORCA v. 4.0.1 software package using the B3LYP5/6-31G[d] approximation [37–39]. Optimization of the singlet ground state geometries was carried out without any restriction on their symmetry.

2.3. Synthesis

General procedure for the Suzuki coupling.

A flask was charged with organoboron precursor, 4,7-dibromo-2,1,3-benzothiadiazole (**11**) and Pd(PPh$_3$)$_4$ (1-5 mol %). The mixture was degassed, toluene, an aqueous solution of Na$_2$CO$_3$ (2.0 M) and ethanol was added and heated to reflux until the reaction was complete. Completeness of the reaction was controlled by GPC analysis. After completion of the reaction, the mixture was cooled down to room temperature, the bottom aqueous phase was taken out by a syringe and organic phase was concentrated and filtrated over a thin pad of silica gel in toluene, which was evaporated by a Rotorvapour.

[5-(4-Bromophenyl)-2-thienyl](trimethyl)silane (4). This compound was obtained by the general procedure for the Suzuki coupling using trimethyl[5-(4,4,5,5-tetramethyl-1,3,2-dioxaborolan-2-yl)-2-thienyl]silane (**2**) (5.74 g, 20.3 mmol), 1,4-dibrombenzene (14.39 g, 61 mmol), Pd(PPh$_3$)$_4$ (70 mg, 0.1 mmol) and aqueous solution (2M) of Na$_2$CO$_3$ (10 ml) in toluene-ethanol mixture (150/10 mL). The reaction mixture was stirred at reflux for 17 hours. The crude product was purified by recrystallization from ethanol to give pure compound **4** as a white solid (4.23 g, 66.8%). ^{1}H NMR (J Hz, CDCl$_3$): δ [ppm] 0.33 (9H, s), 7.20 (1H, d, J = 3.4), 7.34 (1H, d, J = 3.4), 7.48 (4H, s).

Trimethyl[4'-(4,4,5,5-tetramethyl-1,3,2-dioxaborolan-2-yl)biphenyl-4-yl]silane (7). A 1.6 M solution of *n*-butyl lithium (3.2 mL, 5.2 mmol) in hexane was added dropwise to a solution of (4'-bromobiphenyl-4-yl)(trimethyl)silane (**3**) (1.5 g, 4.9 mmol) in anhydrous THF (35 mL), keeping the temperature below -70 °C. The reaction mixture was stirred for 1 hour at -75 °C and IPTMDOB (1.2 g, 6.45 mmol) was added in one portion. The reaction mixture was stirred for 30 min at -78°C and the temperature was slowly allowed to rise to 0 °C. After completion of the reaction, 100 mL of diethyl ether and 100 mL of ice water containing 5 mL of 1 M HCl were added. The organic phase was separated, washed with water, and dried over sodium sulfate. The solvent was evaporated to give 1.8 g of white crystals, containing 82% of compound **7** and

18% of the initial compound **3** (according to GPC). The product was used in the subsequent synthesis without further purification. ^{1}H NMR (J Hz, $CDCl_3$): δ [ppm] 0.30 (9H, s), 1.36 (12H, s), 7.59-7.64 (6H, overlapping peaks), 7.88 (2H, d, J = 7.7).

Trimethyl{5-[4-(4,4,5,5-tetramethyl-1,3,2-dioxaborolan-2-yl)phenyl]-2-thienyl}silane (8). This compound was obtained by the method described above for compound **7** using 1.6 M solution of *n*-butyl lithium in hexane (4 mL, 6.45 mmol), [5-(4-bromophenyl)-2-thienyl](trimethyl)silane (**4**) (3.34 g, 6.0 mmol) and IPTMDOB (1.3 g, 7.0 mmol) in anhydrous THF (100 mL). The product containing 89% of compound **8** according to GPC was used in the subsequent synthesis without further purification. ^{1}H NMR (J Hz, $CDCl_3$): δ [ppm] 0.35 (9H, s), 1.37 (12H, s), 7.23 (1H, d, J = 3.4), 7.44 (1H, d, J = 3.4), 7.63 (2H, d, J = 8.2), 7.82 (2H, d, J = 8.2)

Trimethyl[5'-(4,4,5,5-tetramethyl-1,3,2-dioxaborolan-2-yl)-2,2'-bithien-5-yl]silane (10). This compound was obtained by the method described above for compound **7** using 2.5 M solution of *n*-butyl lithium in hexane (5 mL, 12.6 mmol), 2,2'-bithien-5-yl(trimethyl)silane (**6**) (3 g, 12.6 mmol) and IPTMDOB (2.34 g, 12.6 mmol) in anhydrous THF (60 mL). The product containing 98% of compound **10** according to GPC was used in the subsequent synthesis without further purification. ^{1}H NMR (J Hz, $CDCl_3$): δ [ppm] 0.34 (9H, s), 1.36 (12H, s), 7.14 (1H, d, J = 3.7), 7.23-7.33 (2H, overlapping peaks), 7.53 (1H, d, J = 3.7).

4,7-*Bis*[4'-(trimethylsilyl)biphenyl-4-yl]-2,1,3-benzothiadiazole (F1). This compound was obtained by the general procedure for the Suzuki coupling using compound **7** (8.7 g, 25.9 mmol), 4,7-dibromo-2,1,3-benzothiadiazole (**11**) (3.45 g, 11.7 mmol), $Pd(PPh_3)_4$ (300 mg, 0.26 mmol) and aqueous solution (2M) of Na_2CO_3 (20 mL) in toluene-ethanol mixture (200/20 mL). The reaction mixture was stirred at reflux for 27 hours. The crude product was purified by recrystallization from toluene to give pure compound **F1** as a lime green solid (3.8 g, 55.7%), m_p = 261°C. ^{1}H NMR (J Hz, $CDCl_3$): δ [ppm] 0.34 (18H, s), 7.69 (8H, m, J_1 = 11.6, J_2 = 7.9), 7.81 (4H, d, J = 8.2), 7.88 (2H, s), 8.09 (4H, d, J = 8.2). ^{13}C NMR ($CDCl_3$): δ [ppm] -1.08 126.45, 127.39, 128.02, 129.62, 132.89, 133.92, 136.37, 139.60, 140.97, 141.14, 154.12. ^{29}Si NMR ($CDCl_3$): δ [ppm] -3.90. Anal. Calcd. (%) for $C_{36}H_{36}N_2SSi_2$: C, 73.92; H, 6.20; N, 4.79; S, 5.48%; Si, 9.60. Found: C, 73.87; H, 6.07; N, 4.71; Si, 9.50.

4,7-*Bis*{4-[5-(trimethylsilyl)-2-thienyl]phenyl}-2,1,3-benzothiadiazole (F2). This compound was obtained by the general procedure for the Suzuki coupling using compound **8** (2.5 g, 7.0 mmol), 4,7-dibromo-2,1,3-benzothiadiazole (**11**) (0.92 g, 3.14 mmol), $Pd(PPh_3)_4$ (81 mg, 0.07 mmol) and aqueous solution (2M) of Na_2CO_3 (5 mL) in toluene-ethanol mixture (50/5 mL). The reaction mixture was stirred at reflux for 15 hours. The crude product was purified by recrystallization from toluene-hexane (1:6) mixture to give pure compound **F2** as a yellowish solid (1.4 g, 75%), m_p = 226 °C. ^{1}H NMR (J Hz, $CDCl_3$): *δ* [ppm] 0.38 (18H, s), 7.26 (2H, d, J = 3.4), 7.47 (2H, d, J = 3.5), 7.78-7.87 (6H, overlapping peaks), 8.03 (4H, d, J = 8.5), ^{13}C NMR ($CDCl_3$): δ [ppm] -0.09, 124.75, 126.15, 127.78, 128.19, 128.99, 129.62, 132.67, 134.45, 135.08, 136.28, 140.60, 149.07, 154.05. ^{29}Si NMR ($CDCl_3$): δ [ppm] -6.46. Anal. Calcd. (%) for $C_{32}H_{32}N_2S_3Si_2$: C, 63.38; H, 5.40; N, 4.69; S, 16.11%; Si, 9.41. Found: C, 63.51; H, 5.27; N, 4.74; Si, 9.29.

4,7-*Bis*{5-[4-(trimethylsilyl)phenyl]-2-thienyl}-2,1,3-benzothiadiazole (F3). This compound was obtained by the general procedure for the Suzuki coupling using compound **9** (2.05 g, 5.7 mmol), 4,7-dibromo-2,1,3-benzothiadiazole (**11**) (600 mg, 2.0 mmol), $Pd(PPh_3)_4$ (198 mg, 0.17 mmol) and aqueous solution (2M) of Na_2CO_3 (5 mL) in toluene-ethanol mixture (50/5 mL). The reaction mixture was stirred at reflux for 50 hours. The crude product was purified by recrystallization from toluene-hexane (1:3) mixture to give pure compound **F3** as a red solid (0.89 g, 73%), m_p = 303 °C. ^{1}H NMR (J Hz, $CDCl_3$): *δ* [ppm] 0.31 (18H, s), 7.43 (2H, d, J = 3.8), 7.56 (4H, d, J = 8.0), 7.68 (4H, d, J=8.0), 7.87 (2H, s), 8.11 (2H, d, J = 3.9). ^{13}C NMR ($CDCl_3$): δ [ppm] -1.14, 124.23, 125.16, 125.42, 125.98, 128.76, 133.99, 134.56, 138.86, 140.40, 145.80, 152.73.

^{29}Si NMR (CDCl$_3$): δ [ppm] -3.98. Anal. Calcd. (%) for $C_{32}H_{32}N_2S_3Si_2$: C, 63.38; H, 5.40; N, 4.69; S, 16.11%; Si, 9.41. Found: C, 64.74; H, 5.53; N, 4.46; Si, 9.21.

4,7-*Bis*[5'-(trimethylsilyl)-2,2'-bithien-5-yl]-2,1,3-benzothiadiazole (F4). This compound was obtained by the general procedure for the Suzuki coupling using compound **10** (6.5 g, 17.86 mmol), 4,7-dibromo-2,1,3-benzothiadiazole (**11**) (2.5 g, 8.5 mmol), Pd(PPh$_3$)$_4$ (206 mg, 0.18 mmol) and aqueous solution (2M) of Na_2CO_3 (13.4 mL) in toluene-ethanol mixture (100/10 mL). The reaction mixture was stirred at reflux for 45 hours. The crude product was purified by recrystallization from toluene-hexane (1:1) mixture to give pure compound **F4** as a red solid (3.14 g, 83.1%), m$_p$ = 205 °C. ^{1}H NMR (J Hz, CDCl$_3$): *δ* [ppm] 0.36 (18H, s), 7.18 (2H, d, J = 3.5), 7.28 (2H, d, J = 3.9), 7.35 (2H, d, J = 3.5), 7.82 (2H, s), 8.03 (2H, d, J = 3.9). ^{13}C NMR (CDCl$_3$): δ [ppm] -0.10, 124.70, 125.23, 125.37, 125.73, 128.42, 134.88, 138.26, 138.97, 140.63, 142.33, 152.63. ^{29}Si NMR (CDCl$_3$): δ [ppm] -6.40. Anal. Calcd. (%) for $C_{28}H_{28}N_2S_5Si_2$: C, 55.22; H, 4.63; N, 4.60; S, 26.32; Si, 9.22. Found: C, 55.24; H, 4.69; N, 4.73; Si, 9.22.

3. Results and discussion

3.1. Synthesis

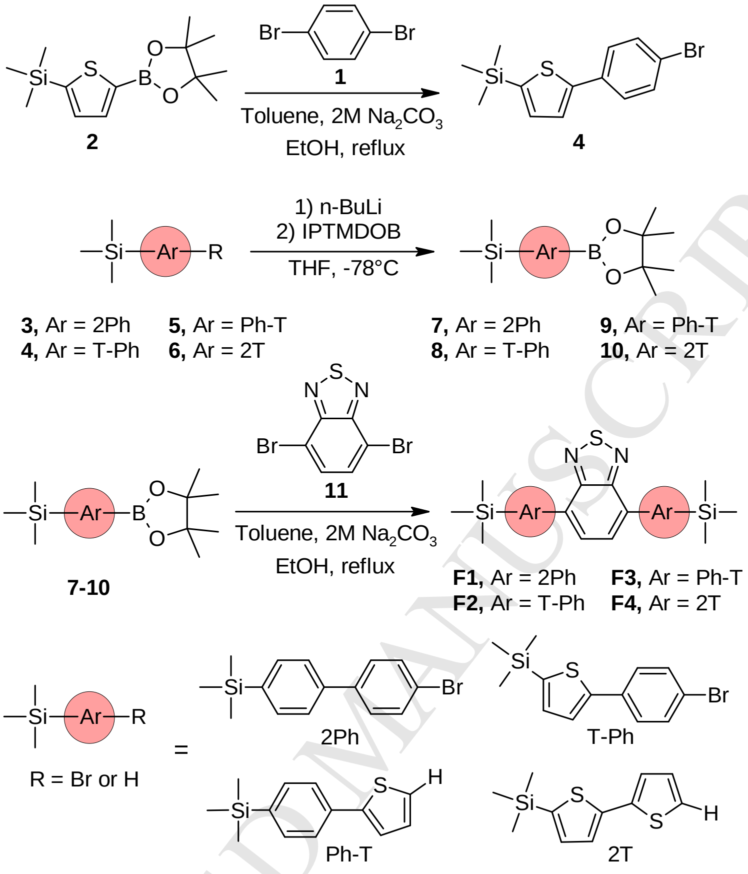

Fig. 2. Scheme of the synthesis of compounds **F1-F4**.

As an object for the study, linear organosilicon BTD-based oligomers in which symmetric donor fragments have different pairs of 1,4-phenylene and 2,5-thiophene units were selected. Their synthesis was carried out in several main steps (Fig.2). First, using various combinations of organometallic and cross-coupling reactions, trimethylsilyl derivatives **3-6** were obtained. The introduction of the trimethylsilyl group was carried out through the reaction of organomagnesium and organolithium precursors with trimethylchlorosilane. Then organoboron precursors **7-10** were obtained and used in the Suzuki cross-coupling reaction with 4,7-dibromo-2,1,3-benzothiadiazole (**11**). After recrystallization, pure compounds **F1-F4** as solids having various colors from lime green to red with the isolated yields of 56-83% were obtained.

GPC, ^{1}H, ^{13}C and ^{29}Si NMR spectroscopy together with the elemental analysis were used to characterize the structure of the intermediates and final compounds (see ESI, Fig. S1-S16). All of them gave satisfactory analysis and spectroscopic data corresponding to their expected molecular structures. In particular, signals of TMS groups in the region of -0.32… -0.38 ppm at ^{1}H NMR spectra, in the region of -0.09 … -1.14 ppm at ^{13}C NMR spectra and in the region of -3.90 … -6.46 ppm at ^{29}Si NMR spectra are present at the corresponding NMR data of compounds **F1-F4**. A detailed description of these data can be found in the Experimental Section. According to the GPC data the purity of all the compounds obtained was higher than 99%.

In the case of compounds **7** and **10**, an attempt was made to obtain the corresponding organosilicon precursors **3** and **6** and corresponding organoboron compounds in a one-pot synthesis from commercially available precursors. This would greatly simplify the preparation of luminophores **F1** and **F4** due to elimination of the purification stage for compounds **3** and **6**. For this purpose, the starting bifunctional 4,4′-dibromobiphenyl and 2,2′-bithiophene were lithiated with one equivalent of n-butyl lithium at -78 °C, stirred for one hour and chlorotrimethylsilane was added in one portion. Slow addition of *n*-butyllithium and keeping temperature of the reaction mixture below -70 °C made it possible to obtain almost completely their monolithium derivatives. After adding of chlorotrimethylsilane and 30 min of stirring at this temperature, GPC analysis showed the formation of 91% and 98% of compounds **3** and **6**, respectively. Thereafter, the second equivalent of *n*-butyllithium solution was added, the reaction mixture was stirred at -78 °C for one hour and IPTMDOB was added in one portion. After isolation, the yield of organoboron precursors **7** and **10** according to GPC analysis was 87% and 96%, respectively. They were used for Suzuki cross-coupling reaction to produce compounds **F1** and **F4**. However, during their purification, it was not possible to eliminate the low-molecular weight impurities. We assume that during the synthesis of compounds **7** and **10**, organoboron precursors without a trimethylsilyl group were also produced as by-products. It was supported by similar absorption spectrum of the low-molecular weight impurities and the final luminophores from 3D GPC analysis using diode array detector. In the case of purification after the separate stage of preparation of organosilicon compounds **3** and **6** during further synthesis of **F1** and **F4** the formation of these impurities was not observed and pure compounds were obtained by simple recrystallization.

3.2. Thermal behavior

Table 1. Thermal properties and solubility of compounds **F1**-**F4**.

Compound	T_m, °C	ΔH, J g^{-1}	ΔS*10^{-3}, J g^{-1} K^{-1}	T_{N2}, °C	T_{air}, °C	S, g L^{-1}
F1	261	73	137	364	358	5.2
F1a	249	100	192	352	332	1.5
F2	226	72	144	370	372	8.5
F3	303	85	148	392	362	1.5
F4	205	63	132	340	357	7.3

T_m - Melting temperature; S - solubility measured in toluene; T_{N2} and T_{air} - decomposition temperature (at 5% weight loss) according to TGA in the inert atmosphere (N_2) and in the air; ΔH - melting enthalpy; ΔS - melting entropy

Thermal properties of the luminophores synthesized were investigated by thermogravimetric analysis (TGA) and differential scanning calorimetry (DSC). According to the TGA data, the 5% weight loss for all the compounds under study both in the air and in the inert atmosphere occurs above 340 °C (Table 1 and Fig. S22-S26 in ESI). This suggest a very high stability of the luminophores investigated both under thermal and thermo-oxidative conditions. Despite the different chemical structure, their decomposition temperatures are close to each other. Bearing in mind high thermal stability of the TMS group, these results suggest that the most thermally unstable fragment in such molecules is the BTD unit. Analyzing dependence of the change in the weight of the sample with increasing temperature (Fig. S22-S26 in ESI), we can conclude that for all these compounds a partial sublimation is characteristic both in an inert atmosphere and in the presence of atmospheric oxygen. This is confirmed by close decomposition temperatures and very low residual weights, even in the inert atmosphere. Introduction of TMS groups does not have any noticeable effect on the stability of the compounds as can be seen from the comparison of the thermal properties of luminophores **F1** and its non-silicon analogue **F1a** (Table 1).

The DSC curves indicate that all these compounds are crystalline (Fig. S17-S21 in ESI). The melting points were determined from the maxima at the first DSC heating scans (Table 1). The subsequent cooling and second heating show similar melting temperatures to those obtained at the first DSC heating scans. Compound **F3** among all the organosilicon compounds investigated has the highest melting point (T_m = 303 °C) and melting enthalpy (ΔH = 85 J g^{-1}). In contrast to the other compounds, it also has the lowest solubility in organic solvents and the largest change in the melting entropy (ΔS = 148 mJ g^{-1} K^{-1}), which also indicates its high degree of crystallinity. The solubility of luminophores **F1**-**F4** correlates well with their melting points. As the solubility increases, the melting temperature decreases. Comparison of compound **F1a** with its organosilicon analogue **F1** showed that the former has the highest melting entropy and entropy. Moreover, its' solubility is 3.5 times lower than those of compound **F1**, which indicates very good solubilizing ability of TMS groups.

3.3. Optical properties

The absorption and PL spectra of **F1-F4** were investigated in diluted THF solutions (Fig.3-4, S27), polystyrene (PS) matrix (Fig.S27-S29 in ESI) and polycrystalline thin films having a thickness of 50-100 nm (Fig.S27, S30-S32 in ESI). The data are summarized in Table 2. On all the absorption spectra of both diluted THF solutions and polycrystalline films there are two absorption bands related to the singlet electron-vibrational transitions – long wavelength and short wavelength. For all molecules, the first peak corresponds to transition $S_0 \rightarrow S_1$. The short wavelength absorption peak corresponds to transition $S_0 \rightarrow S_{1+n}$. In this case, the value of n for all molecules is different and varies from 2 to 5. More detailed information on electron-vibrational transition properties calculated by DFT method is presented in Table S1 in ESI. The distance between these maxima varies from 5000 to 9000 cm^{-1}. The large distance between the maxima observed is typical for the luminophores with a BTD core. The positions of the absorption maxima (λ_{abs}^{max}) and the values of the corresponding molar extinction coefficient (ε_{max}) are given in Table 2.

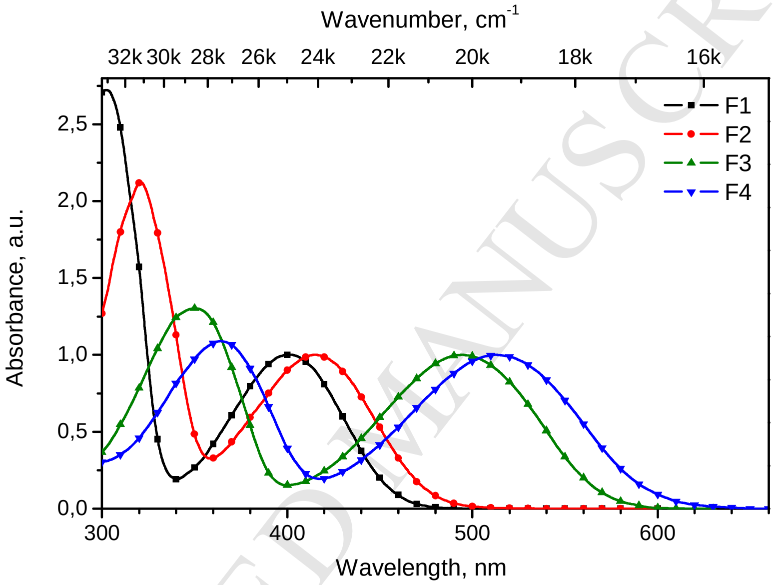

Fig. 3. Absorption spectra of diluted THF solutions of compounds **F1** - **F4**.

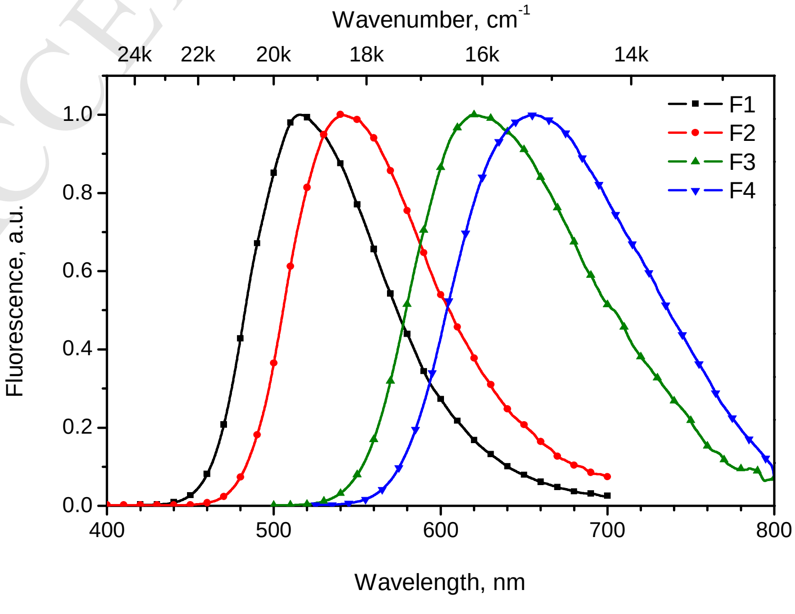

Fig. 4. PL spectra of diluted THF solutions of compounds **F1** - **F4**.

Table 2. Absorption and PL properties of **F1-F4**.

	$\lambda_{abs}^{\max}$, nm			Stokes shift, cm^{-1}			$\varepsilon_{\max}$ *10^3, L mol^{-1} cm^{-1}		$\lambda_{lum}^{\max}$, nm			PLQY ^{a}, %			τ_{PL}, ns	k_{PL} *10^8, s^{-1}
	THF	PS	solid	THF	PS	solid	THF	PS	THF	PS	solid	THF	PS	Solid ^{b}		
F1	401 302	407 307	380 317	5600	4600	6200	21.7 59.2	22 60	516	502	496	84	85	100	5.4	1.56
F1a	399 299	-	-	5500	-	-	20.2 54.6	-	512	-	-	83	-	-	6.0	1.38
F2	415 321	422 325	417 320	5600	4500	4800	27 57.3	26 55.3	540	521	521	73	75	17	4.4	1.65
F3	495 350	502 349	498 355	4100	3600	3700	33.3 43.4	33 42.4	620	611	612	77	66	3	6.9	1.11
F4	513 364	521 368	516 358	4200	3600	4400	32.1 35	30.7 32.6	656	641	668	65	82	3	5.8	1.12

[a] The error in measuring the absolute value of PLQY is ±6%. [b] The relative PLQY calculated with respect to the **F1** sample; $\lambda_{abs}^{\max}$ and $\lambda_{lum}^{\max}$ - absorption and luminescence maxima, respectively; $\varepsilon_{\max}$ - molar extinction coefficient; τ_{PL} - PL lifetime in THF; k_{PL} PL rate constant in THF.

As can be seen from the data presented, the energy of the electronic transitions in the series of BTD-based luminophores depends on the position of the phenylene and thiophene rings relative to the central BTD core. Thus, **F1** with 1,1’-biphenyl fragments has the shortest absorption wavelength, while replacement of the outer phenyl rings by thiophene heterocycles in **F2** leads to a bathochromic shift of the $S_0 \rightarrow S_1$ transition by 800 cm^{-1}, and the $S_0 \rightarrow S_{1+n}$ transition by 2000 cm^{-1}. For its structural isomer **F3**, differing only in the position of the thiophene and phenylene rings, with the thiophene rings adjacent to the BDT core, much greater bathochromic shift is observed: 4700 cm^{-1} for $S_0 \rightarrow S_1$ and 4500 cm^{-1} for $S_0 \rightarrow S_{1+n}$. In the case of **F4** containing 2,2’-bithiophene units, the bathochromic shift is maximal: 5400 cm^{-1} for $S_0 \rightarrow S_1$ and 5600 cm^{-1} for $S_0 \rightarrow S_{1+n}$.

Comparison of the absorption spectrum of diluted THF solutions of the luminophores with a polymer matrix, a slight redshift is observed. At the same time, the molar extinction coefficients hardly change (Table 2, Fig.S27-S29 in ESI). The absorption bands related to the $S_0 \rightarrow S_1$ and $S_0 \rightarrow S_{1+n}$ transitions in the polycrystalline films of compounds **F1-F4** in addition to the main maximum also have a long-wave shoulder (Fig. S30, S32 in ESI). Splitting of the absorption bands can be connected to the resonance interaction of the molecules closely packed in the crystal upon their excitation (Davydov splitting) [40]. Table 3 shows the results of approximating the absorption bands corresponding to the electronic transitions $S_0 \rightarrow S_1$ in **F1-F4** by two Gaussian functions (Fig. S32). The distance between the positions of the functions maxima is 2400 +/- 300 cm^{-1}. The contribution of the long-wavelength peak to the integrated intensity of the absorption band of **F1** molecule is about 2%. In the spectrum of the polycrystalline film of **F2** it reaches 18%, **F3** - 23% and **F4** - 49%. Thus, replacement of the phenylene by thiophene rings in these luminophores leads to a gradual increase in the splitting of the long-wavelength absorption band of the spectra of the polycrystalline films.

Table 3. Splitting of the absorption band for the electronic transition $S_0 \rightarrow S_1$ in polycrystalline films of **F1-F4** by Gaussian functions.

Compound	Peak	Peak maximum position, nm	The fraction of the integrated intensity of the band	Distance between peaks, cm^{-1}
F1	1	379	0.98	2750
	2	423	0.02	
F2	1	413	0.82	2470
	2	460	0.18	
F3	1	507	0.77	2120
	2	568	0.23	
F4	1	491	0.61	2270
	2	552	0.49	

Diluted THF solutions of the luminophores investigated have a bright photoluminescence (Fig.5). Their PL spectra obtained upon excitation by the light with a wavelength corresponding to the position of the maximum of the long-wave band of the absorption in THF are shown in Fig. 4 (for PS matrix and polycrystalline films see Fig.S27, S29 and S31 in ESI). The PL spectra of solutions in THF, polystyrene matrix, and polycrystalline thin films have similar spectral distributions with a single maximum (Fig. S27). A large Stokes shift is observed for all the compounds investigated, which is typical for luminophores based on BTD core. The Stokes shift values for all these compounds ranges from 3600 to 6200 cm^{-1}. For the polymer matrix, the Stokes shift is less than those for the diluted solutions in THF. This effect occurs because upon transition from a diluted THF solution to a polymer matrix the absorption spectrum undergoes a bathochromic and the PL spectrum has a hypsochromic shift.

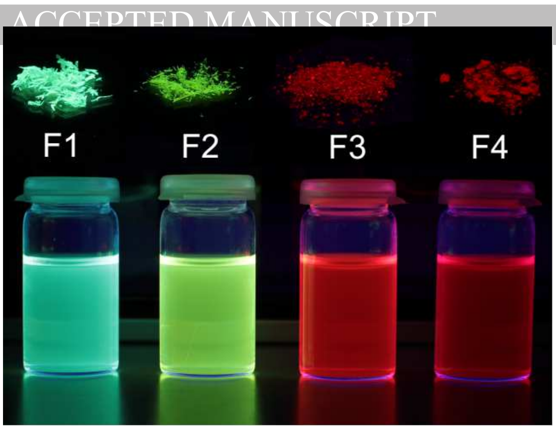

Fig. 5. Photo of 10^{-3}M solutions in THF and powders of **F1**-**F4** illuminated by 365 nm black light.

Table 2 gives the values of the photoluminescence quantum yield (PLQY), which varies from 65 to 84% in THF, and from 66 to 85% in PS matrix. In the case of **F4**, the PLQY increases from 65% in THF solution to 82% in PS matrix. The PL lifetime (τ_{PL}) measured for diluted solutions of the compounds in THF lies in the range of 4.4-6.9 ns. For **F3** and **F4** the PL lifetime is slightly higher than those of **F1** and **F2** molecules. Comparison of the PL rate constant (k_{PL}) values obtained for **F1-F4** molecules according to formula $PLQY = k_{PL} \times \tau_{PL}$ shows that when the phenylene fragment is replaced by a thiophene the PL rate constant is decreased (Table 2).

In polycrystalline thin films, the highest PL intensity has luminophore **F1**. The values of PLQY shown in Table 2 were calculated as a ratio of the integral PL intensity of compounds **F2-F4** to the integral intensity of compound **F1**. The integral PL intensity was calculated according to Formula 1, where $D(\lambda_{ext})$ is the optical density at the excitation wavelength λ_{ext} and $\mathrm{N}_{PL}(\lambda)$ is spectral distribution of PL intensity. The integration was carried out over the entire PL spectrum.

$$\mathrm{I} = \left(1 - 10^{-D(\lambda_{ext})}\right)^{-1} \int_{\Delta\lambda} \mathrm{N}_{PL}(\lambda) d\lambda \qquad (1)$$

In the case of **F2** the relative PLQY in thin polycrystalline film decreases 6 times. In the polycrystalline films of compounds **F3** and **F4** photoluminescence is almost absent. Thus, for the compounds with thiophene fragments (**F2**-**F4**), PL quenching is observed in the aggregated state. This may be due to intrinsic reasons, i.e. by H-aggregation [40], but also by trapping, which is very common in polycrystalline phases [41]. Influence of the terminal TMS groups on the spectral properties was investigated by comparing luminophore **F1** and its non-silicon analogue **F1a** in diluted THF solutions (Fig.6, Table 2). Although the spectra of these compounds are almost similar, a bathochromic shift of the absorption maxima by 125-330 cm^{-1} and of the PL maxima by 150 cm^{-1} is observed. The main influence of the silicon atoms on the absorption spectrum of compound **F1** appears as an increase in the molar extinction coefficient by 10%. The PLQY of both luminophores are very high, 83-84%, and hardly depends on the presence of TMS groups. However, for compound **F1** a higher PL rate constant was found, which can be explained by decrease in the lifetime of the excited state by 10% from 6.0 to 5.4 ns. Thus, the introduction of silicon has a positive effect on both absorption and photoluminescence properties.

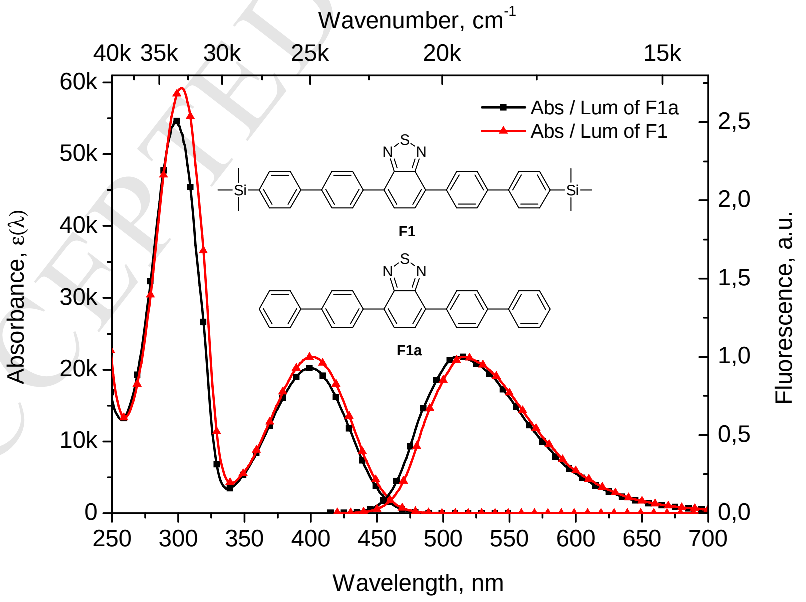

Fig. 6. Absorption and PL spectra of diluted solutions in THF of compounds **F1** and **F1a**.

3.4. Theoretical calculations

Calculated parameters for the organosilicon luminophores using density functional modeling was performed in order to rationalize the observed properties in terms of geometry and electronic structure (Table 4, S1). These data are in a good agreement with the results obtained by optical spectroscopy method: gradual decrease in the energy gap in the transition from phenylene to thiophene derivatives, pronounced donor-acceptor character of the compounds. It was found that the energy gap (E_g) is reduced in the thiophene derivatives **F3** and **F4** when compared to the phenylene compounds **F1** and **F2.** This is mostly due to increase in the highest occupied molecular orbital (HOMO) level together with the electron donating properties of the substituents in benzothiadiazole core. The analogous effect of trimethylsilyl substitution is appeared to be secondary, less in an order of its magnitude.

Table 4. Calculated optimized total energy (E_{tot}), FMO levels and the E_g values for the organosilicon luminophores using density functional modeling (B3LYP/6-31G[d]; ORCA v. 4.0.1).

	E_{tot}, Hatree	**HOMO, eV**	**LUMO, eV**	**E_g, eV**
F1	-2479.1131420	-5.44	-2.32	3.12
F2	-3120.6170309	-5.26	-2.35	2.91
F3	-3120.6102507	-4.98	-2.55	2.43
F4	-3762.1135698	-4.85	-2.58	2.27

The contour orbital diagrams for the frontier molecular orbitals (FMO) are shown in Figure 7. In all cases the lowest unoccupied molecular orbitals (LUMO) is composed mostly on the acceptor BTD fragment. On the other hand, HOMOs show sufficient conjugation between different donor fragments. There are no essential difference observed in the orbital shape caused by the trimethylsilyl substitution.

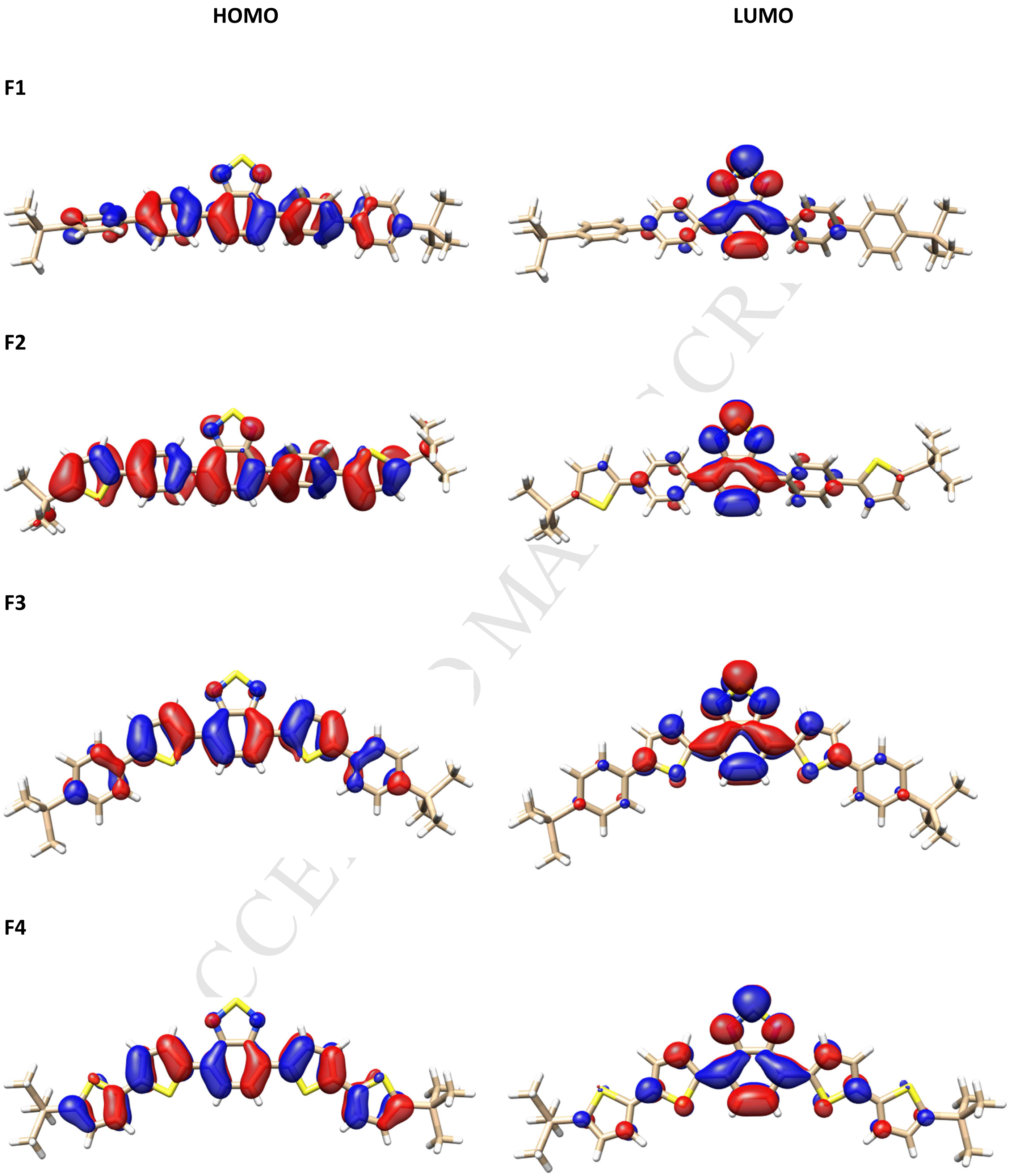

Fig. 7. Diagrams of the frontier orbitals of the **F1**-**F4** (contour values ±0.025).

The influence of the trimethylsilyl substitution upon the energy levels of FMO, as well as upon the E_g gap value, was found to be relevant to control the photophysical properties of the luminophores. For this study DFT calculations of a series of non-TMS analogues of the dyes **F1a** - **F4a** were also performed (see Table S2, Fig. S33). In particular, the E_g gap of the unsubstituted dyes is narrowed in their trimethylsilyl derivatives. This appeared mostly due to the slight increase in the energy of HOMO levels, in its turn uncovering the σ-donor effect of the silyl substituent. The LUMO levels do not show any clear trend under these circumstances.

4. Conclusions

Synthesis of four new conjugated linear oligomers based on BTD electron-accepting core with 4'-(trimethylsilyl)biphenyl-4-yl, 4-[5-(trimethylsilyl)-2-thienyl]phenyl, 5-[4-(trimethylsilyl)phenyl]-2-thienyl and 5'-(trimethylsilyl)-2,2'-bithien-5-yl electron-donating groups is described. Various combinations of thiophene and phenylene fragments in these molecules were used to understand their influence on the absorption-luminescent and thermal properties. It was found that although luminophores **F2** and **F3** are full isomers, their spectral properties are very different. The investigation of absorption and PL spectra has shown that determining factor influencing the spectral characteristics of the luminophores obtained is the nature of the aromatic ring directly attached to the central BTD unit. When the more electron-donating thiophene ring is separated from the BTD core by phenylene ring, its effect on the spectral properties is less prominent than if it is directly connected to the BTD core. This is clearly seen on the properties of isomers **F2** and **F3** when both the absorption and PL maxima are shifted by 2400 cm^{-1} for luminophore **F2** with the thiophene rings adjacent to the BDT core. It is shown that by simply changing the structure of the conjugated donor fragment, it is possible to tune the PL maximum of the luminophores in the 510-660 nm spectral range. All the luminophores investigated show the intensive PL in diluted THF solution and PS polymer matrix with PLQY up to 84-85%, while only **F1** have strong PL in polycrystalline thin film. Apparently, this should be related to the strong interactions in the crystals and particular parking of the molecules containing thiophene rings (H-aggregation), but also by trapping and require further investigations. The introduction of trimethylsilyl groups allows increasing the molar extinction coefficients and accelerating the PL by approximately 10%. At the same time, there is very little effect on the position of absorption and PL maxima and the PL quantum yield. High thermal stabilities of all these compounds having the temperature of 5% decomposition of 340 – 392 °C under nitrogen and 357 – 372 °C in the air, which is partly caused by sublimation, indicate that they can be applied in high temperature optical devices and deposited on the substrate by vacuum sublimation technique. The introduction of trimethylsilyl groups does not affect the thermal stability and extremely increases solubility of the luminophores.

Acknowledgments

This work was performed in the framework of leading science school NSh-5698.2018.3. Synthetic work was supported by Foundation of President of the Russian Federation (project MK- 364.2017.3). Optical properties were studied under support of Russian Science Foundation (grant 15-12-30031). The authors thank G.V. Cherkaev for NMR and P.V. Dmitryakov for TGA and DCS measurements.

Supplementary data

Supplementary data associated with this article such as ^{1}H, ^{13}C and ^{29}Si NMR spectra, TGA and DSC curves and additional spectral figures can be found in the online version.

References

[1] Fyfe D. LED Technology: Organic displays come of age. Nat Photonics 2009;3:453–5. doi:10.1038/nphoton.2009.132.

[2] Bronnbauer C, Osvet A, Brabec CJ, Forberich K. Semitransparent Organic Light Emitting Diodes with Bidirectionally Controlled Emission. ACS Photonics 2016;3:1233–9. doi:10.1021/acsphotonics.6b00234.

[3] Kajii H, Ohtomo T, Ohmori Y. Electroluminescence emission patterns of organic light-emitting transistors based on crystallized fluorene-type polymers. Jpn J Appl Phys 2017;56:03BA01. doi:10.7567/JJAP.56.03BA01.

[4] Zaumseil J, Donley CL, Kim J-S, Friend RH, Sirringhaus H. Efficient Top-Gate, Ambipolar, Light-Emitting Field-Effect Transistors Based on a Green-Light-Emitting Polyfluorene. Adv Mater 2006;18:2708–12. doi:10.1002/adma.200601080.

[5] Gwinner MC, Vaynzof Y, Banger KK, Ho PKH, Friend RH, Sirringhaus H. Solution-Processed Zinc Oxide as High-Performance Air-Stable Electron Injector in Organic Ambipolar Light-Emitting Field-Effect Transistors. Adv Funct Mater 2010;20:3457–65. doi:10.1002/adfm.201000785.

[6] Uekert T, Solodovnyk A, Ponomarenko S, Osvet A, Levchuk I, Gast J, et al. Nanostructured organosilicon luminophores in highly efficient luminescent down-shifting layers for thin film photovoltaics. Sol Energy Mater Sol Cells 2016;155:1–8. doi:10.1016/j.solmat.2016.04.019.

[7] Wang Z, Liu Q, Chen T, Wang Y, Yuan J, Zheng C, et al. Molecular rearrangement at charged states: Intrinsic effects upon photo and electroluminescence. Dye Pigment 2015;113:529–35. doi:10.1016/j.dyepig.2014.09.017.

[8] DaSilveira Neto BA, Lopes AS, Ebeling G, Gonçalves RS, Costa VEU, Quina FH, et al. Photophysical and electrochemical properties of π-extended molecular 2,1,3-benzothiadiazoles. Tetrahedron 2005;61:10975–82. doi:10.1016/j.tet.2005.08.093.

[9] Jadhav T, Dhokale B, Patil Y, Mobin SM, Misra R. Multi-Stimuli Responsive Donor–Acceptor Tetraphenylethylene Substituted Benzothiadiazoles. J Phys Chem C 2016;120:24030–40. doi:10.1021/acs.jpcc.6b09015.

[10] Li Y, Scudiero L, Ren T, Dong W-J. Synthesis and characterizations of benzothiadiazole-based fluorophores as potential wavelength-shifting materials. J Photochem Photobiol A Chem 2012;231:51–9. doi:10.1016/j.jphotochem.2012.01.011.

[11] Fang H, Gao H, Wang T, Zhang B, Xing W, Cheng X. Benzothiadiazole-based D-π-A-π-D fluorophores: Synthesis, self-assembly, thermal and photophysical characterization. Dye Pigment 2017;147:190–8. doi:10.1016/j.dyepig.2017.07.045.

[12] Hou J, Chen H-Y, Zhang S, Li G, Yang Y. Synthesis, Characterization, and Photovoltaic Properties of a Low Band Gap Polymer Based on Silole-Containing Polythiophenes and 2,1,3-Benzothiadiazole. J Am Chem Soc 2008;130:16144–5. doi:10.1021/ja806687u.

[13] Kim J, Park SH, Cho S, Jin Y, Kim J, Kim I, et al. Low-bandgap poly(4H-cyclopenta[def]phenanthrene) derivatives with 4,7-dithienyl-2,1,3-benzothiadiazole unit for photovoltaic cells. Polymer (Guildf) 2010;51:390–6. doi:10.1016/j.polymer.2009.12.009.

[14] Liu J, Bu L, Dong J, Zhou Q, Geng Y, Ma D, et al. Green light-emitting polyfluorenes with improved color purity incorporated with 4,7-diphenyl-2,1,3-benzothiadiazole moieties. J Mater Chem 2007;17:2832. doi:10.1039/b700004a.

[15] Thomas KRJ, Huang T-H, Lin JT, Pu S-C, Cheng Y-M, Hsieh C-C, et al. Donor-Acceptor Interactions in Red-Emitting Thienylbenzene-Branched Dendrimers with Benzothiadiazole Core. Chem - A Eur J 2008;14:11231–41. doi:10.1002/chem.200801694.

[16] Carvalho PHPR, Correa JR, Guido BC, Gatto CC, De Oliveira HCB, Soares T a, et al.

Designed benzothiadiazole fluorophores for selective mitochondrial imaging and dynamics. Chemistry 2014;20:15360–74. doi:10.1002/chem.201404039.

[17] Bohra H, Wang M. Direct C–H arylation: a “Greener” approach towards facile synthesis of organic semiconducting molecules and polymers. J Mater Chem A 2017;5:11550–71. doi:10.1039/C7TA00617A.

[18] Aldakov D, Palacios MA, Anzenbacher P. Benzothiadiazoles and Dipyrrolyl Quinoxalines with Extended Conjugated Chromophores−Fluorophores and Anion Sensors. Chem Mater 2005;17:5238–41. doi:10.1021/cm050985p.

[19] Zhang X, Yamaguchi R, Moriyama K, Kadowaki M, Kobayashi T, Ishi-i T, et al. Highly dichroic benzo-2,1,3-thiadiazole dyes containing five linearly π-conjugated aromatic residues, with fluorescent emission ranging from green to red, in a liquid crystal guest–host system. J Mater Chem 2006;16:736. doi:10.1039/b512493j.

[20] Bonillo B, Sprick RS, Cooper AI. Tuning Photophysical Properties in Conjugated Microporous Polymers by Comonomer Doping Strategies. Chem Mater 2016;28:3469–80. doi:10.1021/acs.chemmater.6b01195.

[21] Neto B a D, Lapis A a M, Da Silva Júnior EN, Dupont J. 2,1,3-benzothiadiazole and derivatives: Synthesis, properties, reactions, and applications in light technology of small molecules. European J Org Chem 2013:228–55. doi:10.1002/ejoc.201201161.

[22] Luh T, Cheng Y. Alternating divinylarene–silylene copolymers. Chem Commun 2006:4669–78. doi:10.1039/B609412K.

[23] Ohshita J. Group 14 metalloles condensed with heteroaromatic systems. Org Photonics Photovoltaics 2016;4:52–9. doi:10.1515/oph-2016-0006.

[24] Ponomarenko SA, Kirchmeyer S. Conjugated Organosilicon Materials for Organic

Electronics and Photonics, 2010, p. 33–110. doi:10.1007/12_2009_48.

[25] Skorotetcky MS, Borshchev O V., Surin NM, Odarchenko Y, Pisarev SA, Peregudova SM, et al. Synthesis and photostability of 1,4- bis (5-phenyloxazol-2-yl)benzene (POPOP) structural isomers and their trimethylsilyl derivatives. Dye Pigment 2017;141:128–36. doi:10.1016/j.dyepig.2017.02.006.

[26] Starikova TY, Surin NM, Borshchev O V., Pisarev SA, Svidchenko EA, Fedorov Y V., et al. A novel highly efficient nanostructured organosilicon luminophore with unusually fast photoluminescence. J Mater Chem C 2016;4:4699–708. doi:10.1039/C6TC00979D.

[27] Shumilkina EA, Borshchev O V., Ponomarenko SA, Surin NM, Pleshkova AP, Muzafarov AM. Synthesis and optical properties of linear and branched bithienylsilanes. Mendeleev Commun 2007;17:34–6. doi:10.1016/j.mencom.2007.01.014.

[28] Shigehiro T, Yagi S, Maeda T, Nakazumi H, Fujiwara H, Sakurai Y. Novel 10,13-disubstituted dipyrido[3,2-a:2′,3′-c]phenazines and their platinum(II) complexes: highly luminescent ICT-type fluorophores based on D–A–D structures. Tetrahedron Lett 2014;55:5195–8. doi:10.1016/j.tetlet.2014.07.069.

[29] Urben P, editor. Bretherick's Handbook of Reactive Chemical Hazards. 7th ed. Boston: Elsevier; 2006.

[30] Lane F. Clinton, Gray W. Kramer. Handling air-sensitive reagents. Aldrichimica Acta 1977;10:11–6.

[31] Cameo chemicals n.d. https://cameochemicals.noaa.gov/unna/1298.

[32] Safe handling of chlorosilanes 2003:26. http://www.silicones.eu/uploads/chlorosilanes-manual-22082003.pdf.

[33] Zhu E, Hai J, Wang Z, Ni B, Jiang Y, Bian L, et al. Two-Dimensional Polyfluorenes Bearing Thienylenevinylene π-Bridge-Acceptor Side Chains for Photovoltaic Solar Cells. J Phys Chem C 2013;117:24700–9. doi:10.1021/jp4072718.

[34] Hanss D, Wenger OS. Conformational Effects on Long-Range Electron Transfer: Comparison of Oligo- p -phenylene and Oligo- p -xylene Bridges. Eur J Inorg Chem 2009;2009:3778–90. doi:10.1002/ejic.200900396.

[35] Hasegawa M, Kobayakawa K, Matsuzawa H, Nishinaga T, Hirose T, Sako K, et al. Macrocyclic Oligothiophene with Stereogenic [2.2]Paracyclophane Scaffolds: Chiroptical Properties from π-Transannular Interactions. Chem - A Eur J 2017;23:3267–71. doi:10.1002/chem.201605842.

[36] Crosby GA, Demas JN. Measurement of photoluminescence quantum yields. Review. J Phys Chem 1971;75:991–1024. doi:10.1021/j100678a001.

[37] Hertwig RH, Koch W. On the parameterization of the local correlation functional. What is Becke-3-LYP? Chem Phys Lett 1997;268:345–51. doi:10.1016/S0009-2614(97)00207-8.

[38] Hirata S, Head-Gordon M. Time-dependent density functional theory within the Tamm–Dancoff approximation. Chem Phys Lett 1999;314:291–9. doi:10.1016/S0009-2614(99)01149-5.

[39] Neese F. The ORCA program system. Wiley Interdiscip Rev Comput Mol Sci 2012;2:73–8. doi:10.1002/wcms.81.

[40] Gierschner J, Park SY. Luminescent distyrylbenzenes: tailoring molecular structure and crystalline morphology. J Mater Chem C 2013;1:5818. doi:10.1039/c3tc31062k.

[41] Gierschner J, Lüer L, Milián-Medina B, Oelkrug D, Egelhaaf H-J. Highly Emissive H-Aggregates or Aggregation-Induced Emission Quenching? The Photophysics of All-Trans

para -Distyrylbenzene. J Phys Chem Lett 2013;4:2686–97. doi:10.1021/jz400985t.